Article

Spatiotemporal Distribution Characteristics and Influencing Factors of Freeze–Thaw Erosion in the Qinghai–Tibet Plateau

Zhenzhen Yang [1], Wankui Ni [1,*], Fujun Niu [2], Lan Li [3] and Siyuan Ren [1]

1   College of Geological Engineering and Geomatics, Chang'an University, Xi'an 710054, China; 2022026044@chd.edu.cn (Z.Y.)
2   State Key Laboratory of Frozen Soil Engineering, Northwest Institute of Eco-Environment and Resources, Chinese Academy of Sciences, Lanzhou 730000, China; niufujun@lzb.ac.cn
3   College of Architecture and Engineering, Huanghuai University, Zhumadian 463000, China
*   Correspondence: niwankui@chd.edu.cn

Abstract: Freeze–thaw (FT) erosion intensity may exhibit a future increasing trend with climate warming, humidification, and permafrost degradation in the Qinghai–Tibet Plateau (QTP). The present study provides a reference for the prevention and control of FT erosion in the QTP, as well as for the protection and restoration of the regional ecological environment. FT erosion is the third major type of soil erosion after water and wind erosion. Although FT erosion is one of the major soil erosion types in cold regions, it has been studied relatively little in the past because of the complexity of several influencing factors and the involvement of shallow surface layers at certain depths. The QTP is an important ecological barrier area in China. However, this area is characterized by harsh climatic and fragile environmental conditions, as well as by frequent FT erosion events, making it necessary to conduct research on FT erosion. In this paper, a total of 11 meteorological, vegetation, topographic, geomorphological, and geological factors were selected and assigned analytic hierarchy process (AHP)-based weights to evaluate the FT erosion intensity in the QTP using a comprehensive evaluation index method. In addition, the single effects of the selected influencing factors on the FT erosion intensity were further evaluated in this study. According to the obtained results, the total FT erosion area covered 1.61×10^6 km^2, accounting for 61.33% of the total area of the QTP. The moderate and strong FT erosion intensity classes covered 6.19×10^5 km^2, accounting for 38.37% of the total FT erosion area in the QTP. The results revealed substantial variations in the spatial distribution of the FT erosion intensity in the QTP. Indeed, the moderate and strong erosion areas were mainly located in the high mountain areas and the hilly part of the Hoh Xil frozen soil region.

Keywords: freeze-thaw erosion; Qinghai–Tibet Plateau; AHP; GIS; spatiotemporal characteristics

1. Introduction

Freeze–thaw (FT) erosion is the whole process of expansion or contraction of water in soil or rock due to temperature changes in alpine regions, which causes mechanical damage to the geotechnical body and the consequent transport, migration and accumulation of broken material [1,2]. In fact, FT erosion is mainly distributed in frozen soils, with a global total area of permafrost of about 3.74×10^7 km^2 and a seasonal frozen soil area of about 1.04×10^8 km^2 [3], accounting for 25% and 69% of the global land area, respectively. Freeze–thaw (FT) erosion is the third largest type of soil erosion in China after water and wind erosion [4–6], occurring mostly in regions with high latitudes, high altitudes, and cold climates [7]. Several effects can result from FT erosion, including changes in the nature of soils [8,9] and the weakening of their resistance to erosion [10]. Moreover, FT erosion-derived products can increase sediment contents in rivers, seriously affecting the ecological and hydrological environment of the Changjiang–Yellow Rivers. In this study, we mapped the classified evaluation of FT erosion intensity on the QTP, aiming to provide

a reference for the prevention and control of soil FT erosion in the region as well as regional ecological environment protection and restoration.

Although FT erosion is one of the major soil erosion types in cold regions, most of the previous studies have focused on wind and water erosion, and relatively few studies have been conducted on FT erosion. However, in recent years, with global warming, thermokarst-like phenomena such as thaw slumps, rock glaciers, and FT mudflows have occurred frequently in the frozen zone [11,12]. Its disastrous effects and environmental and engineering impacts are becoming increasingly significant, but there is still a lack of quantitative assessment studies on these phenomena. Zhang and Liu [13] proposed a new method to define the FT erosion area in Tibet in 2005, and qualitatively analyzed the distribution pattern of FT erosion in Tibet based on GIS software. Ouyang [14] analyzed the intensity and area of FT erosion in the Yarlung Zangbo River basin in the last 20 years using the visual interpretation method in 2014. Guo [15] established an FT erosion estimation model based on seven factors in 2015 and concluded that the average erosion intensity of the QTP was moderate. Lu [16] introduced the indicator of soil sand content in 2021 and analyzed the spatiotemporal distribution characteristics of the FT erosion in Jinsha in the Yalong and Lancang Rivers using a comprehensive weighted evaluation model. In addition, several researchers have studied the intensity levels and spatial distribution characteristics of the FT erosion in the Buha River Basin [17] and Sanjiangyuan area [18,19], as well as the degrees and responses of single factors to FT erosion sensitivity [20]. However, most related studies have considered only four to six factors for evaluating FT erosion, including temperature, precipitation, slope degree, slope aspect, vegetation coverage and soil texture, which are not sufficient to comprehensively assess the influencing factors of FT erosion. Permafrost has developed in 40.32% of the total area of the QTP. In addition, the remaining part of the QTP area is a deep-seasonal permafrost zone, presenting a series of FT geomorphology types with repeated actions. Hence, it is essential to consider the influences of FT erosion in the frozen soil area of the QTP.

The QTP is an inland plateau in Asia known as the "Roof of the World" and the "Third Pole". It represents the largest and highest plateau in China and worldwide, respectively [21]. The QTP is a typical FT erosion area in China due to its high latitude, high altitude, and low temperature [22]. Indeed, the QTP includes the largest and most extensive permafrost area in the world's low and middle latitudes [23], accounting for about 49.3% and 5% of the permafrost area in China and worldwide, respectively [24]. In this context, 11 factors were selected in this study to assess the intensity and spatial distribution characteristics of FT erosion in the QTP using ArcGIS 10.7 software, including not only the seven basic influencing factors of FT erosion, namely the annual temperature difference (ATD), annual mean precipitation (AMP), slope degree, slope aspect, elevation, vegetation coverage (NDVI), and soil–sand content, but also four additional factors, including maximum freezing depths (MFD), active layer thicknesses (ALT), thaw slumps, and rock glaciers. The analytic hierarchy process was first performed to calculate the weights of each parameter and then a multi-factor comprehensive evaluation of FT erosion in the QTP was carried out using a comprehensive evaluation index method. In addition, a single-factor impact analysis was conducted using ArcGIS software. The present study provides a reference for the prevention and control of soil FT erosion in the QTP region, as well as for regional ecological environmental protection and restoration.

2. Study Area and Data Sources

2.1. Study Area

The QTP is the largest plateau in China and the highest in the world, with a range and average altitude of 2400–8500 m and over 4000 m, respectively. It is located between latitude and longitude ranges of 25°49′N–39°50′N and 73°30′E–104°42′E, respectively, covering a total area of about 2.63×10^6 km^2 and accounting for about one-fourth of China's total land area. This plateau includes the entire Tibet Autonomous Region of China, most of Qinghai Province, the southern part of the Xinjiang Uygur Autonomous Region, the western part

of Sichuan Province, and parts of Yunnan and Gansu provinces (Figure 1). The QTP is characterized by low air temperatures, which decrease with increasing altitude and latitude. The average annual temperature in the hinterland of the plateau is lower than 0 °C, with high ATDs (12.6–29.2 °C) and daily temperature differences. In addition, there is a high regional variability in precipitation in the study area, with precipitation increasing from northwest to southeast and the AMP ranging from 3 to 877 mm. The QTP is densely populated with mountains of varying altitudes and large slopes, with a maximum slope degree of about 49.67°. The terrain is steep and complex, showing high and low terrain characteristics in the western and eastern parts of the QTP. The plateau is characterized by rarefied air, abundant light, snow-capped mountains, and intense solar radiation. The permafrost zone of the QTP covers an area of about 1.06×10^6 km^2 [25], accounting for about 40.32% of the total area of the QTP. The thickness of the permafrost zone ranges from 1.27 to 4.0 m, with a seasonal frozen soil area of about 1.46×10^6 km^2 [25], accounting for about 55.54% of the total area of the QTP. The MFD of the seasonal frozen soil area ranges from 6 to 258 cm.
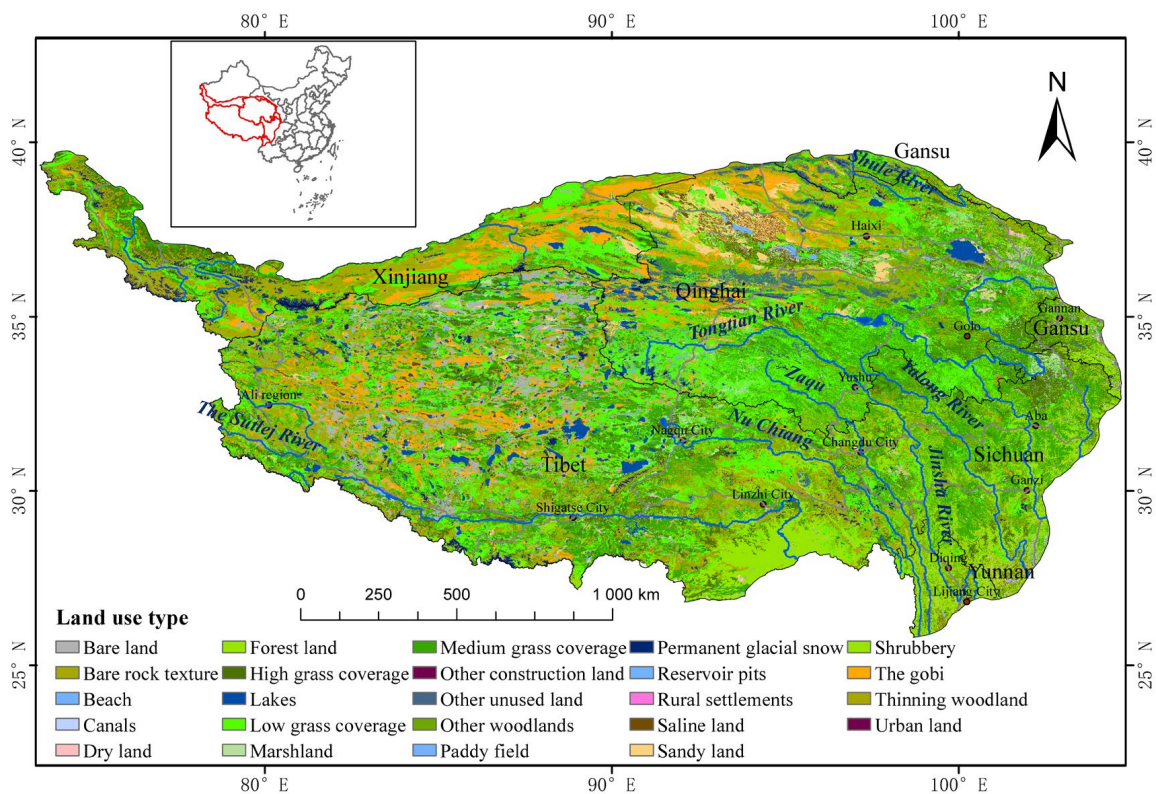
Figure 1. Land use types in the QTP.

Figure 1 shows the different land use types in the QTP. The main land use type in the study area is grassland, with an area of about 1.27×10^6 km^2, accounting for 48.46% of the total area of QTP. This is followed by bare land and rocky areas with an area of 4.81×10^5 km^2 (18.31% of the total area of the QTP), followed by forest, sand/Gobi desert, and lake/glaciers/snow areas, with total surface areas of 3.46×10^5, 3.24×10^5, and 1.37×10^5 km^2, accounting for 13.15%, 12.33%, and 5.19% of the total area of the QTP, respectively.

2.2. Data Sources

The data sources used in this study are shown in Table 1. All the data were collected in 2020 and resampled to a 1 km resolution.

Table 1. Data sources.

Data	Type	Resolution/m	Data Sources/DOI Number	Data Producer
Land use type	Raster	30	https://doi.org/10.12078/2018070201 (accessed on 15 June 2004)	Xu and Liu
Elevation	Raster	1000	https://www.resdc.cn/data.aspx?DATAID=123 (accessed on 15 June 2004)	Shuttle Radar Topography Mission-SRTM 90 m
Vegetation coverage	Raster	1000	https://www.resdc.cn/data.aspx?DATAID=342 (accessed on 15 June 2004)	SPOT/VEGETATION PROBA-V 1 KM PRODUCTS
Sand content	Raster	1000	https://www.resdc.cn/data.aspx?DATAID=260 (accessed on 15 June 2004)	Resource and Environmental Science Data Platform
Annual temperature difference	Raster	1000	https://data.tpdc.ac.cn/zh-hans/data/71ab4677-b66c-4fd1-a004-b2a541c4d5bf (accessed on 4 September 2018)	Ding and Peng 2020
Annual mean precipitation	Raster	1000	https://data.tpdc.ac.cn/zh-hans/data/faae7605-a0f2-4d18-b28f-5cee413766a2 (accessed on 4 September 2018)	Ding and Peng 2020
Maximum freezing depth	Raster	1000	https://data.tpdc.ac.cn/zh-hans/data/3794b246-515a-4506-85a3-95d092c23f63 (accessed on 4 September 2018)	Wang and Ran 2021
Active layer thickness	Raster	1000	https://doi.org/10.1016/j.accre.2021.08.009 (accessed on 27 December 2021)	Yin and Niu 2021
Thaw slump	Vector	/	https://data.tpdc.ac.cn/zh-hans/data/ccfb2902-6e44-4033-b6f6-b76b16e28157 (accessed on 4 September 2018)	Luo and Niu 2022
Rock glacier	Vector	/	https://data.tpdc.ac.cn/zh-hans/data/584ab5ed-91ee-47a8-9a20-f1e493b5e1c9 (accessed on 4 September 2018)	Wang and Lin 2023

3. Research Methods

3.1. Identification of the FT Erosion Areas

The FT erosion zone is defined as the area where the FT action is the main camping force, characterized by specific FT erosion geomorphology [16]. In fact, to define whether an area is a freeze–thaw erosion zone, it must be determined whether the erosion dynamics of the area are mainly caused by freeze–thaw action [18,26]. There must be FT erosion in the FT erosion zone, but the areas where FT erosion occurs may not necessarily belong to the FT erosion zone, because areas where FT erosion occurs may not necessarily be dominated by FT erosion [13]. The most recognized and widely accepted method for determining the extent of the FT erosion zone is to consider the lower boundary of the ice-marginal zone as the lower boundary of the FT erosion zone, as proposed by Zhang et al. in 2005 [13,16,27–30]. However, the lower boundary of the ice-marginal zone is about 200 m lower than the lower boundary of the permafrost zone [13]. Therefore, the lower boundary of the FT erosion zone for QTP is calculated as shown in Equation (1):

$$H = \frac{66.3032 - 0.9197Y - 0.1438X + 2.5}{0.005596} - 200 \tag{1}$$

where *H* denotes the elevation of the lower boundary of the FT erosion zone (m); *X* and *Y* denote the longitude (°E) and latitude (°N), respectively.

ArcGIS software was employed to extract the FT erosion areas according to the digital elevation model (DEM) data of the QTP. Specifically, the extraction was carried out using the following steps: (1) The DEM raster data of the QTP were converted to points; (2) the XY coordinates of each point were added; (3) field H was added and the field calculator was used to calculate according to Equation (1); (4) points with DEM ≥ H were selected

by attributes, and then exported and converted to raster; the same raster size that is the same as the DEM data was selected. The FT areas were determined according to the land use type data, excluding the glaciers and desert areas. The spatial distribution of the FT erosion areas in the QTP is shown in Figure 2.
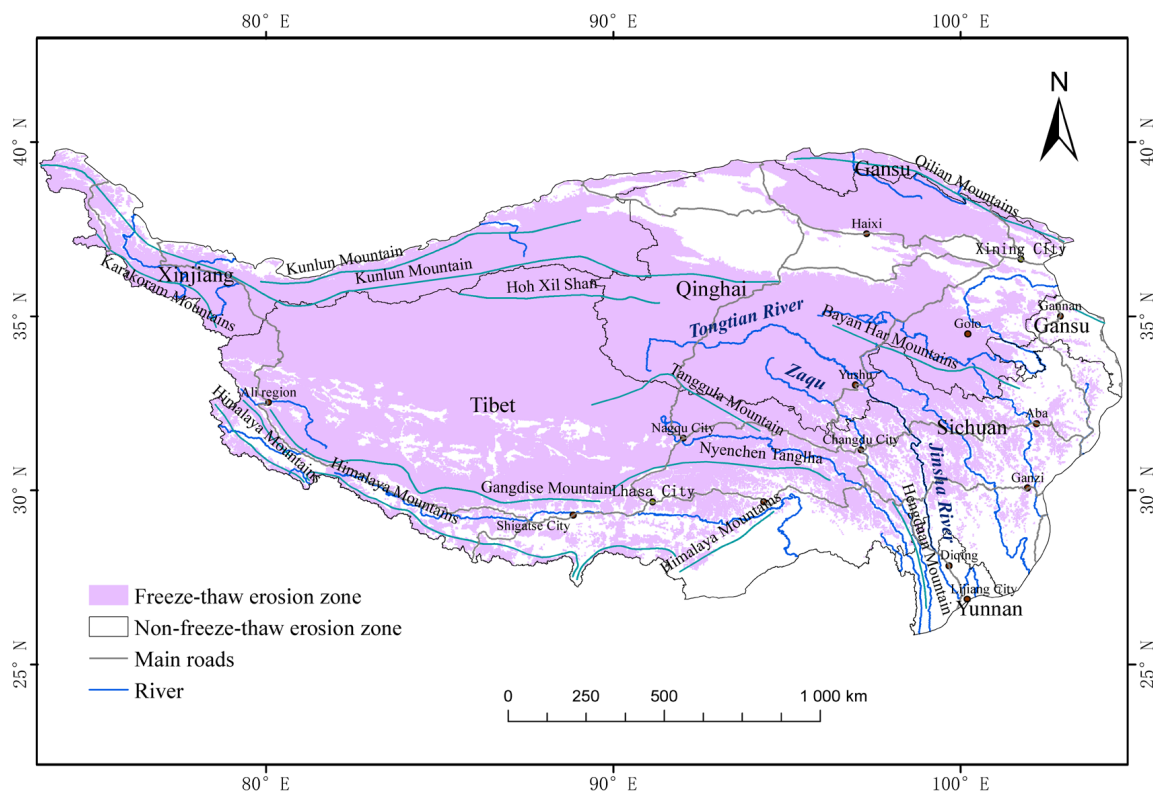
Figure 2. Distribution of the freeze–thaw erosion areas in the QTP.

3.2. Freeze–Thaw Erosion Evaluation Factors

3.2.1. Meteorological and Vegetation Factors

(1)   Annual temperature difference

In this study, the annual temperature difference (ATD) data were used to assess the spatial distribution of FT erosion in the QTP. Periodic changes in soil temperatures are an important factor triggering and affecting FT erosion [31]. Indeed, periodic changes in temperatures can affect the FT erosion degrees. The depth of frozen soil layers can increase with decreasing temperature. On the other hand, the higher the temperatures, the greater the thickness of the thawed soil layers. Therefore, the occurrence risk of FT erosion can increase with the increasing temperature difference. In particular, the amplitude and frequency of temperature changes near 0 °C can seriously affect the physical properties of soils and their resistance to erosion events [32]. However, there was a lack of soil temperature data in the study area due to the severe climatic environment [33]. However, Zhou found a strong correlation between soil and air temperatures [34], explaining the extensive use of air temperature data in previous related studies that substitute soil temperatures. The ATD refers to the difference between the highest and lowest average monthly temperatures in a given year. The highest and lowest average monthly temperatures on QTP in 2020 were observed in August and February, respectively. The ATD data of the study area are shown in Figure 3a.

(**a**)

(**b**)

(**c**)

(**d**)

(**e**)

(**f**)

(**g**)

(**h**)

Figure 3. *Cont.*

(i)

(j)

(k)
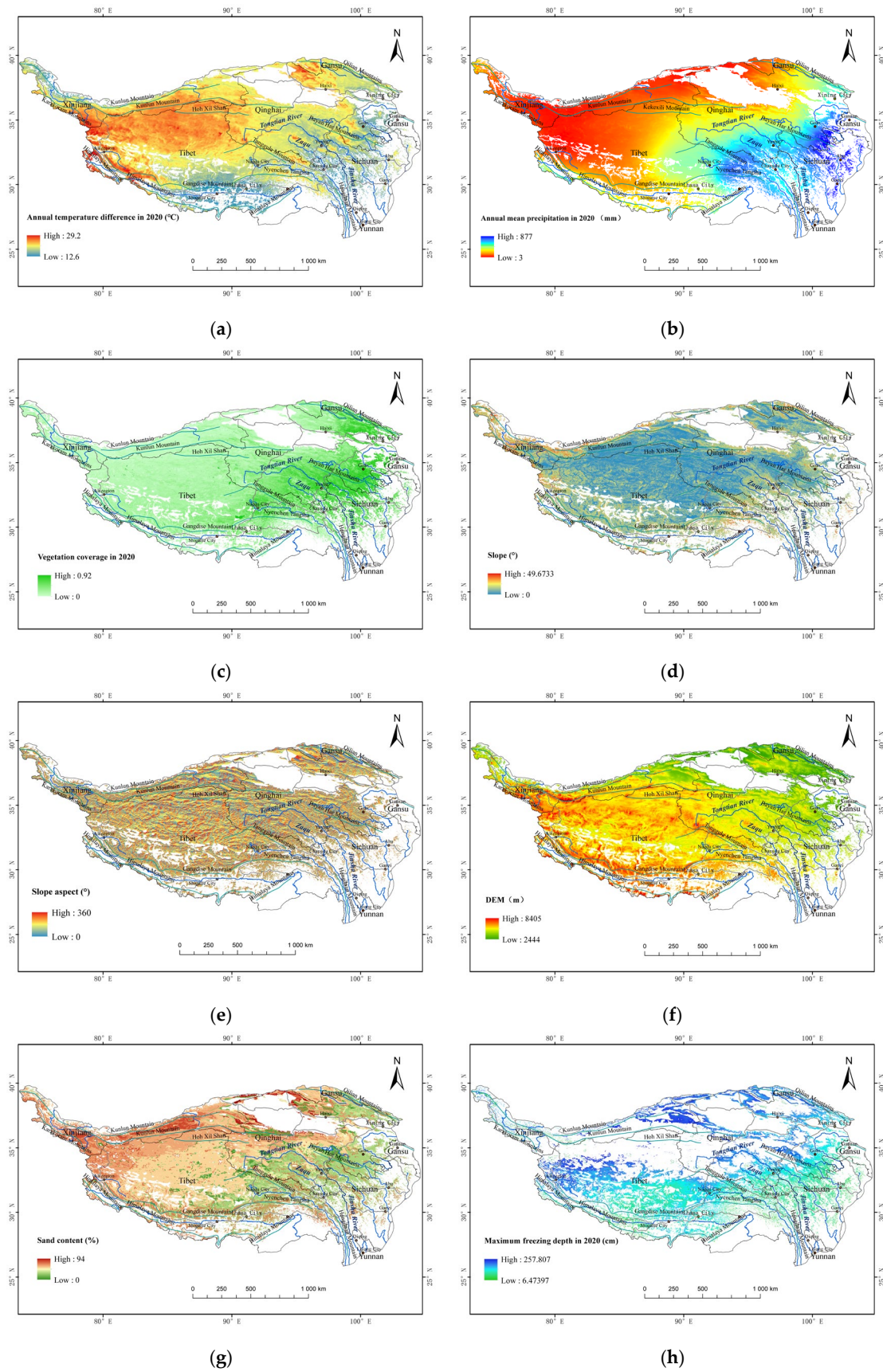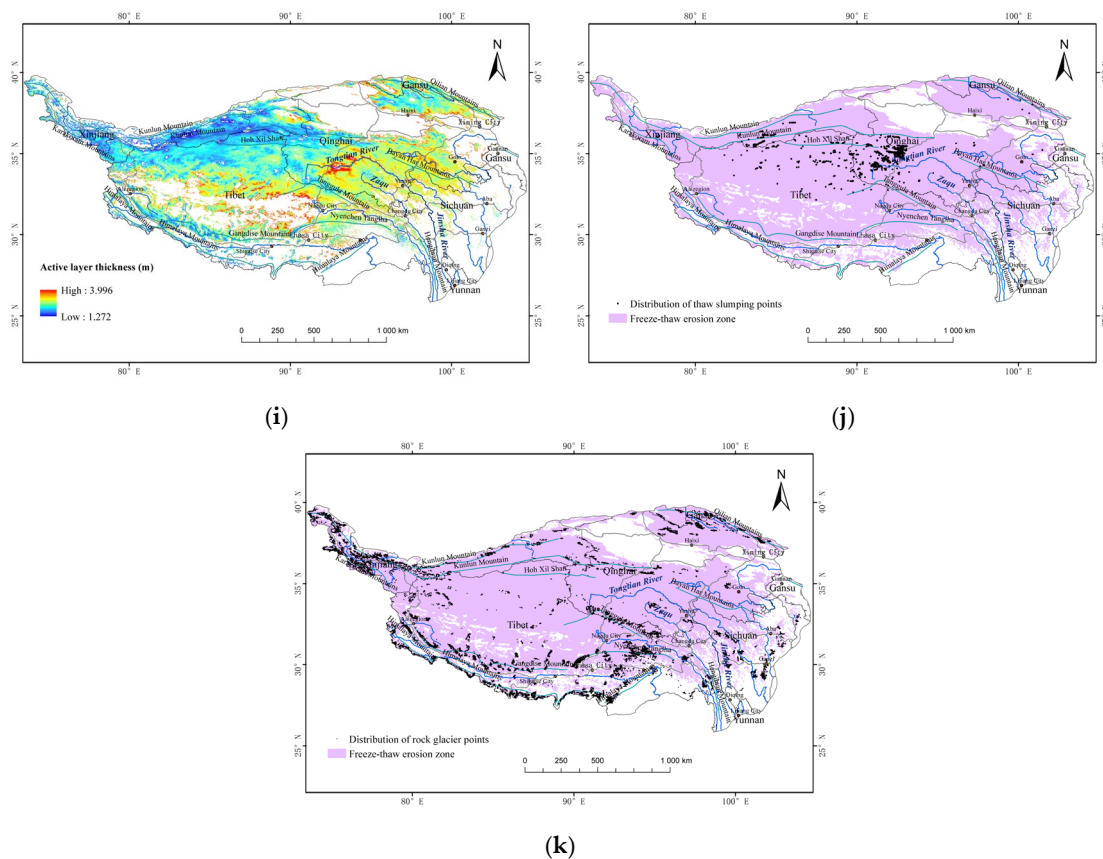
Figure 3. Spatial distributions of the 11 freeze–thaw erosion factors in the QTP. (**a**) Annual temperature difference. (**b**) Annual mean precipitation. (**c**) Vegetation coverage. (**d**) Slope. (**e**) Slope aspect. (**f**) Elevation. (**g**) Sand content. (**h**) Maximum freezing depth. (**i**) Active layer thickness. (**j**) Distribution of the thaw slumping points. (**k**) Distribution of the rock glacier points.

(2) Annual mean precipitation

Precipitation is a major factor influencing FT erosion in soils, especially in arid and semi-arid regions [35], providing a material source for FT erosion. Precipitation has not only a scouring effect on soil surfaces but can also increase soil water contents, enhancing damage effects on soils under freezing and thawing conditions [36]. In addition, precipitation can directly affect the physical properties of soils, which, in turn, affect the resistance of soils to erosion events [1]. The specific precipitation data of the QTP were extracted from those of China. The annual mean precipitation data of the study area are shown in Figure 3b.

(3) Vegetation coverage

Vegetation coverage (NDVI) is one of the main influencing factors of FT erosion. Unlike other influencing factors, vegetation can significantly weaken FT erosion [37]. The presence of vegetation can reduce soil temperature differences, while the above-ground part and root systems of vegetation can protect the soil surface and stabilize soils, respectively [20]. Therefore, the higher the NDVI, the weaker the FT erosion effect. The NDVI data of the study area were extracted from the vegetation index data of China (Figure 3c).

3.2.2. Topography and Geomorphology

(1) Slope

Slope can be used to reflect the degrees of influences of topography on FT erosion. Indeed, slope can mainly affect the transport distance and material amounts derived from FT erosion. Generally, the degrees, transport distances, and material amounts of FT erosion

events increase with the increasing slope [38]. The slope data of the study area were extracted in this study from the DEM data using ArcGIS software. The slope data of the study area are shown in Figure 3d.

(2)   Slope Aspect

Slope aspect is an important factor reflecting the influence of topography on FT erosion. Spatial differences in slope aspects can result in different FT erosion degrees. Zhang et al. [1] highlighted stronger solar radiation on sunny slopes than those on shady slopes, indicating comparatively higher evaporation rates, temperature changes, and FT erosion degrees than those on shady slopes. However, thaw slumps on permafrost slopes in the Hoh Xil hilly mountain area are dominated by north and northeast-facing slopes [11]. In addition, an investigation study on the FT-altered accumulations along the Sichuan–Tibet Railway highlighted dominant accumulations on the north-facing slopes [39]. Therefore, the slope aspects of the study area were assigned different weights reflecting their importance in the FT erosion assessment (Table 2). The slope aspect data were extracted from the DEM data of the QTP using ArcGIS software. The spatial distribution of the slope aspect in the study area is shown in Figure 3e.

Table 2. Specific weights of the slope aspect angle data.

Angle	0–45°	45–90°	90–135°	135–180°	180–225°	225–270°	270–315°	315–360°
Value	0.75	0.75	0.25	0.20	0	0.3	0.5	0.6

(3)   Elevation

The altitude of the QTP ranges from 2400 to 8500 m, indicating an obvious altitude difference. In general, the higher the altitudes, the lower the soil temperatures and the stronger the FT erosion degrees [38]. The elevation data of the QTP were extracted in this study from the DEM data of China using ArcGIS software. The elevations of the study area are shown in Figure 3f.

3.2.3. Geological Factors

(1)   Soil Texture

Soil texture is an important influencing factor of FT erosion, reflecting the combination of soil particles of different sizes and diameters. According to the international classification standards of soils, sands refer to soil particles with sizes ranging from 0.02 to 2 mm. Indeed, sandy soils are characterized by larger soil particles than those of silt and clay particles, making them more susceptible to erosion events [16]. In fact, the resistance of soil to erosion events can be substantially weakened with increasing soil–sand particle proportion, thereby enhancing the FT erosion effect. In this study, the soil–sand content data were extracted from the soil texture data of China. The spatial distribution of the soil–sand contents in the study area is shown in Figure 3g.

(2)   Maximum freezing depth

Maximum freezing depths (MFD) of soil are the maximum value of the thickness of the frozen soil layer, measured from the surface downwards, in seasonally frozen soil zones [40]. Seasonally frozen soils or rocks are layers that thaw and freeze at surfaces in summer and winter, respectively [41]. The MFD of seasonally frozen soil areas are positively correlated with FT erosion intensity. The MFD data were extracted in this study from the data set of MFD of 1 km seasonal frozen soil per decade in Northwest China, Tibet and surrounding areas (Figure 3h).

(3)   Active layer thickness

The active layer represents the overlying layer of soil that thaws in summer and freezes in winter as a permafrost zone. Permafrost is defined as a permanently frozen soil layer with a continuous temperature at or below 0 °C for at least two consecutive years [42]. The greater the thickness of the active layer in a permafrost zone, the lower the permafrost stability, and the greater the thickness of the active layer of soil involved in the FT process, thereby enhancing the FT erosion intensity. The data for active layer thickness were obtained by downloading simulated data on the thickness and ground temperature of the active layer of permafrost on the QTP over many years. The spatial distribution of the active layer thickness in the study area is shown in Figure 3i.

3.2.4. Freeze–Thaw-Related Factors

In this study, thaw slumps and rock glaciers were selected as FT factors. Their point densities were used to assess the FT erosion intensity. The data were processed using the following methods: element to point–point density analysis. The thaw slump and rock glacier data downloaded for use in this paper are based on field surveys and the artificial visual interpretation of high-resolution remote sensing images. Artificial visual interpretation is an important means of geoscientific analysis, which has a relatively high dependence on interpreters. Interpreters are required to have field work experience as well as the ability to analyze remote sensing information and logical reasoning. On this basis, the interpretation is carried out according to the morphology, color tone, texture, shadow and other characteristic features of the features on the remote sensing image. Remote sensing data used to interpret thaw slumps and rock glaciers have spatial resolutions of 10–100 m and 1–10 m, respectively, covering the entire QTP, reflecting the observations of thaw slumps and rock glaciers on the QTP and avoiding errors caused by sampling bias or uneven observation points.

(1)   Thaw slump activity

Thaw slumping refers to the phenomenon of gravitational melting and collapsing of overburdens through sloping areas, where thick surface ice is distributed due to anthropogenic- or natural factor-induced increases in temperatures [11]. Thaw slumping is one of the main types of FT erosion. Indeed, the increasing thaw slumping indicates that FT erosion is stronger in a certain area. The spatial distribution of thaw slumping in the study area is shown in Figure 3j [43].

(2)   Rock glaciers

Rock glaciers are multi-year frozen geological bodies consisting of frozen weathered debris or moraines slowly sliding through valleys or slopes under the actions of gravity and freeze–thaw cycles [44]. These debris are, in fact, called rock glaciers because of their tongue- or lobe-shaped forms similar to those of glaciers. However, its surface is free of exposed ice bodies. Rock glaciers are also one of the main types of FT erosion. The high densities of rock glacier points in an area indicate strong FT erosion. The spatial distribution of the rock glaciers in the study area is shown in Figure 3k [45].

3.3. Determination of the Factor Weights for Evaluating Freeze–Thaw Erosion

There are many methods for determining the weights of FT erosion evaluation factors, which can be roughly categorized into subjective and objective weighting methods. At present, the commonly used weight determination methods mainly include expert scoring, analytic hierarchy process, and entropy weight methods. The Analytic Hierarchy Process is a multi-objective decision analysis method that combines qualitative and quantitative analysis methods. It is widely used because of the advantages of high flexibility and obvious system hierarchy. In this study, we calculated the specific weights of each influencing factor of FT erosion using the analytic hierarchy process by Yaahp 10.1 software, taking into account the characteristics of the study area, according to the following steps: (1) Establish a hierarchical structure model. Organize and hierarchize the problem to be solved, and add

decision objectives, intermediate level elements and alternatives, respectively. (2) Construct all judgment matrices in each level. The numbers 1-9 and their reciprocals are used as scales to define the judgment matrices, as shown in Table 3. (3) Conduct a hierarchical single sorting and consistency test. Calculate the consistency ratio CR; when CR < 0.1, the consistency of the judgment matrix is considered acceptable; otherwise, appropriate corrections should be made to the judgment matrix. (4) Conduct a hierarchical total ordering and consistency test.

Table 3. Importance scale for judgment matrices.

b_{ij} Cale	Meaning
1	Indicates that b_i is as important as b_j
3	Indicates that b_i is slightly more important than b_j
5	Indicates that b_i is more important than b_j
7	Indicates that b_i is very important than b_j
9	Indicates the extreme importance of b_i over b_j
2, 4, 6, 8	Denotes the middle value of the above neighboring scales
1/2, 1/4, 1/7, 1/8	Denotes the reciprocal of the judgment value of b_i and b_j

The evaluation hierarchy model of FT erosion strength constructed in this paper is shown in Figure 4. The judgment matrix of the evaluation indexes is shown in Tables 4–8, which is taken according to the judgment matrix importance scale (Table 3), synthesizing the observations of the study area as well as the previous research results. According to Figure 4 as well as Tables 3–8, using Yaahp software, the specific weights of each evaluation factor were finally calculated, as shown in Table 9.
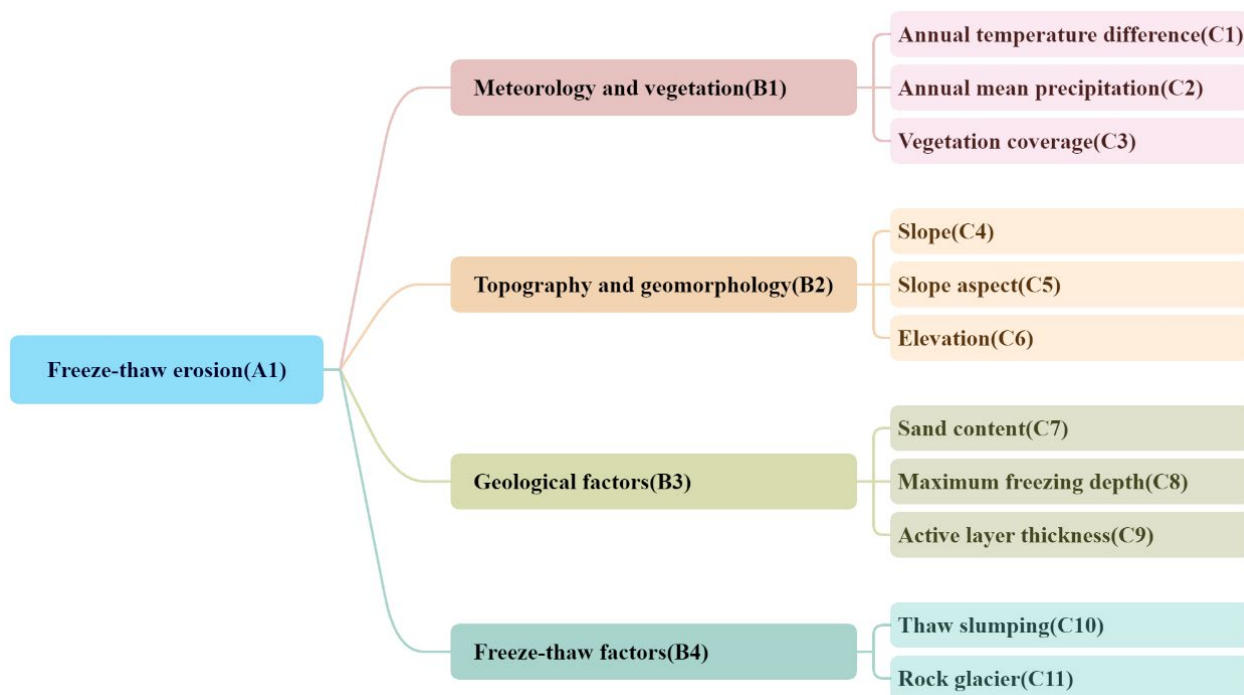
Figure 4. Hierarchical model for evaluation of freeze–thaw erosion strength in Yaahp software.

Table 4. Judgment matrix for the classification and evaluation of the FT erosion intensity in the QTP (CR = 0.0227).

Evaluation Indicators	B1	B2	B3	B4
B1	1	1	1	1/2
B2		1	1/2	1/2
B3			1	1
B4				1

Note: B1 refers to meteorology and vegetation; B2 refers to topography and geomorphology; B3 refers to geological factors; B4 refers to freeze–thaw factors.

Table 5. Judgment matrix of the meteorological and vegetation indicators (CR = 0.0516).

Meteorological and Vegetation Factors (B1)	C1	C2	C3
C1	1	1	2
C2		1	1
C3			1

Note: C1 refers to the annual temperature difference; C2 refers to annual mean precipitation; C3 refers to vegetation coverage.

Table 6. Judgment matrix of the topographic and geomorphologic indicators (CR = 0.0237).

Topographical and Geomorphological Factors (B2)	C4	C5	C6
C4	1	5	2
C5		1	1/4
C6			1

Note: C4 refers to the slope; C5 refers to the slope aspect; C6 refers to the elevation.

Table 7. Judgment matrix of the geological indicators (CR = 0.0019).

Geological Factors (B3)	C7	C8	C9
C7	1	1/7	1/8
C8		1	1
C9			1

Note: C7 refers to the sand content; C8 is the maximum freezing depth; C9 refers to the active layer thickness.

Table 8. Judgment matrix of the freeze–thaw influencing factors (CR = 0.0000).

Freeze–Thaw Influencing Factors (B4)	C10	C11
C10	1	1
C11		1

Note: C10 refers to thaw slumping; C11 refers to rock glaciers.

Table 9. Analytic hierarchy process (AHP)-based weights of the evaluation factors.

Factor Types	Weights	Influencing Factors	Weights
B1	0.2048	C1	0.0842
		C2	0.0671
		C3	0.0535
B2	0.1690	C4	0.0960
		C5	0.0166
		C6	0.0565
B3	0.2881	C7	0.0181
		C8	0.1320
		C9	0.1380
B4	0.3381	C10	0.1690
		C11	0.1690

3.4. Evaluation of the Freeze–Thaw Erosion Intensity

A comprehensive evaluation index method was employed in this study to evaluate the FT erosion intensity in the QTP, combining the selected influencing factors to ensure a single intensity index. In this study, the selected factors were first standardized before using the analytic hierarchy process to calculate the specific weight of each influencing factor. Finally, a comprehensive evaluation formula was used to evaluate the FT erosion intensity in the QTP using ArcGIS software.

3.4.1. Index Normalization

Standardization is crucial to reduce the error caused by different units and scales of different evaluation indicators [19]. Hence, the selected influencing factors were normalized in this study to dimensionless data ranging from 0 to 1 using a standardization method. The factors contributing to the FT erosion process (ATD, AMP, slope, elevation, sand content, MFD, ALT, thaw slumping point density, and rock glacier point density) were normalized in a forward direction (Equation (2)); the slope aspect data were assigned values for each angle according to Table 1. On the other hand, the restricting factor (NDVI) of the FT erosion process was normalized in the opposite direction (Equation (3)). All the selected factors were normalized using the following formulas [46]:

$$I_i = \frac{I - I_{min}}{I_{max} - I_{min}} \tag{2}$$

$$I_i = \frac{I_{max} - I}{I_{max} - I_{min}} \tag{3}$$

where I_i denotes the normalized value of each factor; I denotes the actual value of each factor; I_{min} and I_{max} denote the minimum and maximum values of each factor, respectively.

3.4.2. Comprehensive Evaluation Index Method

The comprehensive evaluation formula is as follows:

$$F = \sum_{i=1}^{n} W_i I_i \Big/ \sum_{i=1}^{n} W_i \tag{4}$$

where F denotes the comprehensive evaluation index of the FT erosion intensity; n denotes the number of the selected evaluation factors; W_i denotes the weight of each evaluation factor; I_i denotes the normalized value of each evaluation factor.

The higher the F value, the stronger the FT erosion intensity.

3.5. Validation Method

As the intensity of FT erosion in QTP is obtained in this paper, different colors are used to represent different degrees of FT erosion. Moreover, the data for comparison and validation are also in different colors to represent the volume of soil erosion caused by thaw slumps and the results of the susceptibility to thaw slumps, respectively. Therefore, this paper adopts the per-pixel comparison method for comparison verification. Per-pixel comparison involves analyzing each pixel in corresponding positions between two images to determine differences in color. At its core, per-pixel comparison evaluates the color difference between pixels in corresponding positions in two images. The basic idea is to measure how much the color of each pixel in one image deviates from the color of the corresponding pixel in the other image.

The method has the following main steps: Begin by loading the two images that you want to compare and ensure that the images are of the same dimensions so that corresponding pixels can be compared directly; convert the images to different color spaces according to your requirements; for each pixel, obtain the corresponding pixel in the other image by accessing the pixel at the same coordinates; once you have the color

values of corresponding pixels from both images, calculate the color difference between them; apply a threshold to the calculated differences to determine whether two pixels are considered similar or different; interpret the results to draw conclusions about the similarity or difference between the two images.

4. Results

4.1. Comprehensive Evaluation of the Freeze–Thaw Erosion Intensity

According to the obtained results, the FT erosion area in the QTP covered 1.61×10^6 km^2, accounting for 61.33% of the total area of the QTP. The calculated evaluation index of the FT erosion intensity in the QTP ranged from 0.0061 to 0.5112. In this study, the natural breaks classification method was used to categorize the comprehensive evaluation index of the FT erosion intensity into four classes, namely micro, mild, moderate, and strong FT erosion intensity classes, corresponding to FT erosion index ranges of 0.0061–0.1857, 0.1857–0.2310, 0.2310–0.2843, and 0.2843–0.5112, respectively (Figure 5).
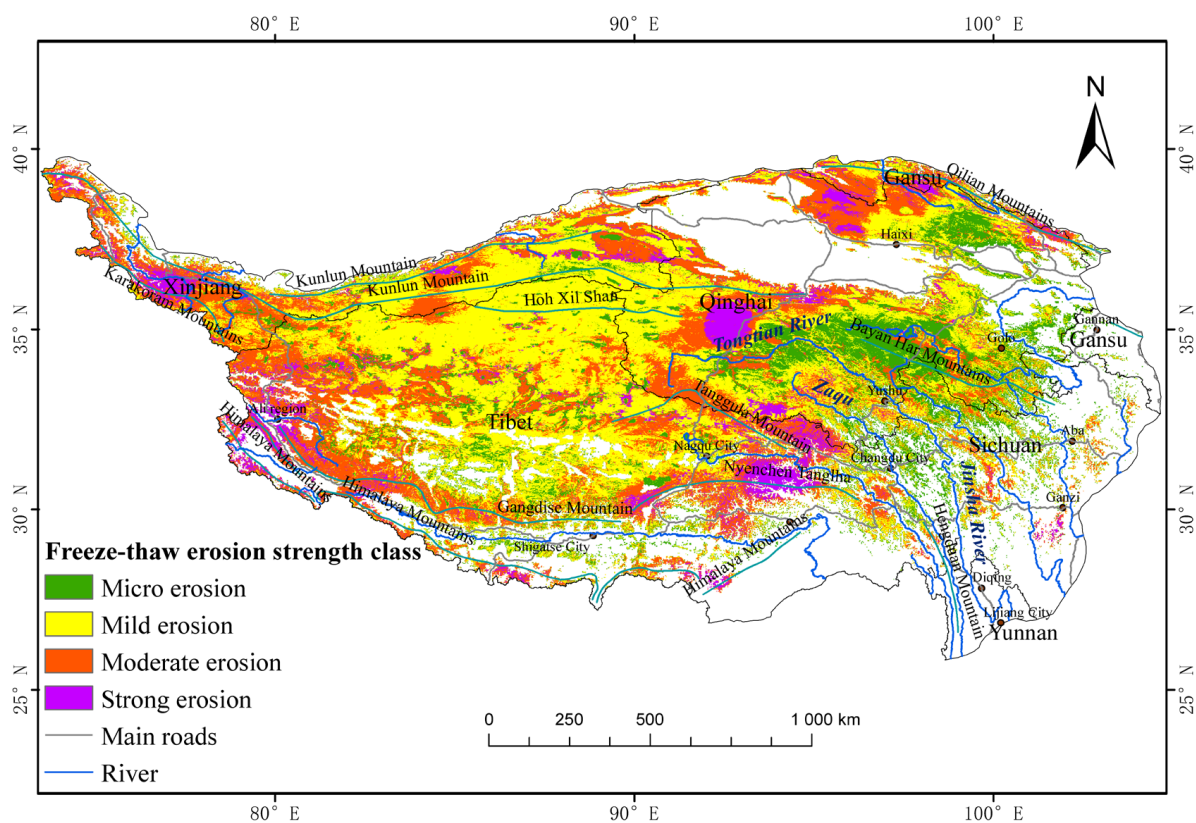
Figure 5. Classification of the freeze–thaw erosion intensity in the study area.

The results of the comprehensive FT erosion evaluation in the QTP are shown in Table 10. The results showed a dominance of the mild and moderate FT erosion classes in the study area, with total areas of 7.33×10^5 and 4.94×10^5 km^2, accounting for 45.44 and 30.65% of the total FT erosion area in the study area, respectively. The micro FT erosion intensity was the third most dominant class, followed by the strong FT erosion intensity class, with total areas of 2.61×10^5 and 1.25×10^5 km^2, accounting for 16.19% and 7.72% of the total FT erosion areas in the study area, respectively.

The results revealed substantial variations in the spatial distribution of the different FT erosion intensities in the study area. The moderate and strong FT erosion classes were mainly distributed in the high mountain areas and the Hoh Xil frozen soil of the hilly region. These areas are, in fact, characterized by low AMP and NDVI, as well as comparatively higher ATDs, slopes, elevations, soil–sand contents, MFDs, and ALTes than those in the other parts. The FT erosion strength class is higher under the combined effect of these

factors. The mild FT erosion class was mainly distributed in the Tibet Autonomous Region in the western and central parts of the QTP. These parts are characterized by comparatively higher ATDs, AMPs, elevations, and lower NDVI, but lower slopes and ALTes than those in the other parts of the study area. The southeastern part of the Qinghai–Tibet Plateau is mainly slightly eroded, and the intensity of freeze–thaw erosion along rivers or near roads is generally slightly higher. The region has small ATDs, small elevations, large NDVI, low soil–sand content, and small MFDs.

Table 10. Comprehensive evaluation results of the FT erosion intensity in the QTP.

Erosion Class	Erosion Intensity	Area (10^4 km^2)	Proportion (%)
Non-FT erosion zone	/	101.66	/
Micro erosion	0.0061–0.1857	26.10	16.19
Mild erosion	0.1857–0.2310	73.26	45.44
Moderate erosion	0.2310–0.2843	49.41	30.65
Strong erosion	0.2843–0.5112	12.45	7.72

4.2. Verification of the Freeze–Thaw Erosion Intensity Results

To validate the findings of this paper, the data on thaw slumps on the QTP studied by Jiao et al. [47] as well as Yin et al. [48] were selected for comparative validation. Figure 6 shows the comparison results of the thaw slumping-induced soil erosion in the QTP [47] and those revealed in the present study, showing roughly consistent research results. The Hoh Xil region exhibited the high FT erosion intensity class due to its location in the hinterland of the QTP, where scattered spatial FT erosion was observed (Figure 7). However, due to the gentle slopes in some parts of the Hoh Xil region, its erosion volume varies in size. Figure 8 shows the results of the thaw-slump susceptibility in the QTP [48] and the results of this present study. The results showed higher thaw-slump susceptibility and FT erosion intensities in the Hoh Xil hilly region than those in the other parts of the QTP. In addition, high FT erosion intensities were observed in the same areas where thaw-slump susceptibility was observed, showing a significant plateau characteristic. In addition, in-site investigations demonstrated a high accuracy of the obtained results.
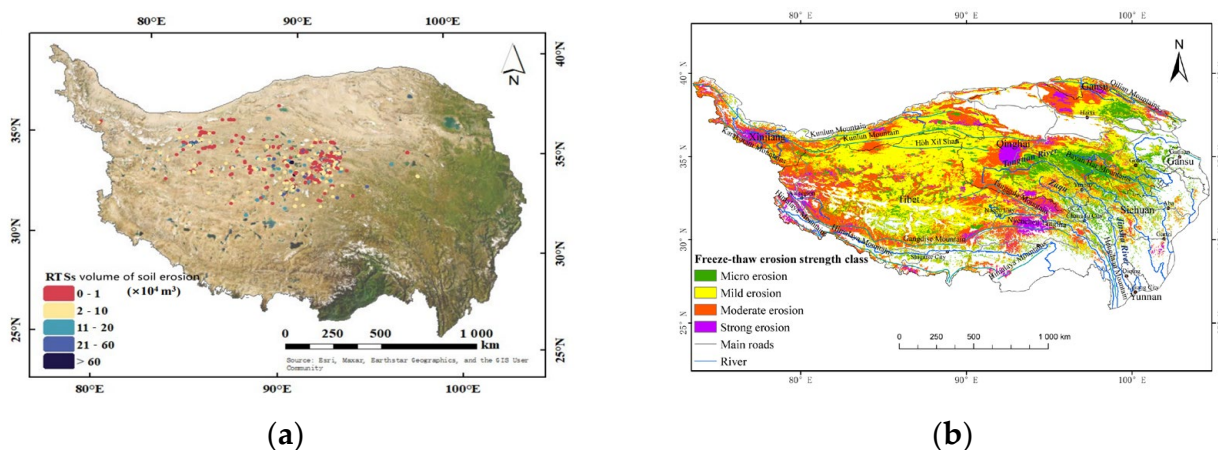
Figure 6. Comparison of the obtained freeze–thaw erosion results in the QTP. Volumes of soil erosion revealed by Jiao [47] (**a**); research results of this article (**b**).

Figure 7. Freeze–thaw erosion in the Hoh Xil region.

(**a**)

(**b**)
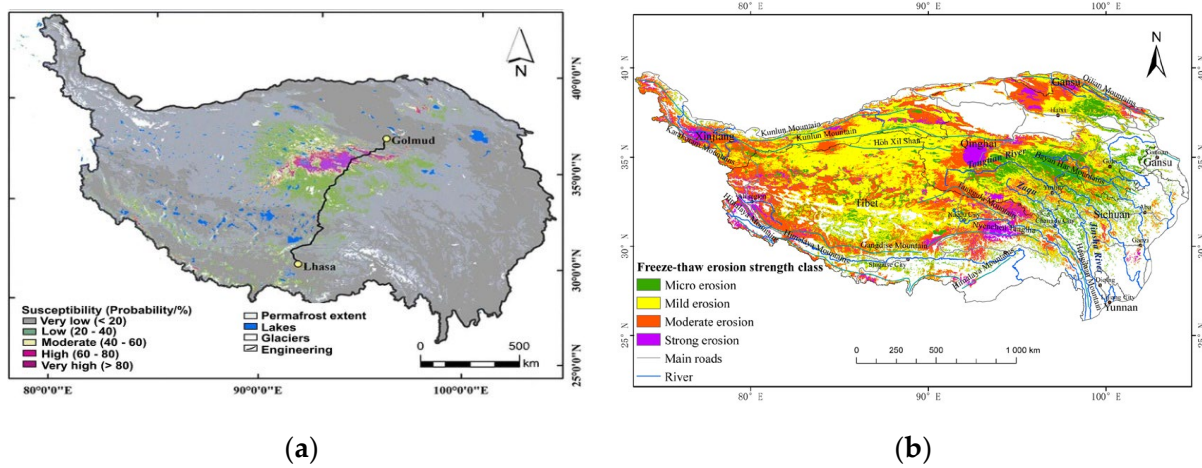
Figure 8. Comparison of the obtained freeze–thaw erosion results in the QTP. Thaw slump susceptibility revealed by Yin [48] (**a**); research results of this article (**b**).

4.3. Single Factor Impact Assessment

In order to further explore the relationship between the spatial distribution of the FT erosion intensity and each single factor in the QTP, the remaining 9 indicators were superimposed on the FT erosion layer using ArcGIS software, excluding thaw slumping and rock glaciers. The specific steps were as follows: (1) the indicator data were reclassified (e.g., ATD); (2) the freeze–thaw erosion class maps and reclassified ATD data were rasterized to surface; (3) the FT erosion data were intersected with ATD; (4) the obtained data were imported using Excel statistics. Grading of the evaluation indicators according to Table 11.

Table 11. Grading scale for evaluation indicators.

Influence Factor	Classification of Indicators			
Annual temperature difference/°C	12.6–19.2	19.2–21.5	21.5–23.6	23.6–29.2
Annual mean precipitation/mm	3–130	130–282	282–451	451–877
Vegetation coverage	0–0.16	0.16–0.36	0.36–0.62	0.62–0.92
Slope/°	0–3.30	3.30–7.57	7.57–13.58	13.58–49.68
Elevation/m	2444–4166	4166–4741	4741–5232	5232–8405
Sand content/%	0–38	38–57	57–73	73–94
Maximum freezing depth/cm	6–100	100–142	142–181	181–258
Active layer thickness/m	1.27–1.96	1.96–2.39	2.39–2.94	2.94–4.0
Slope aspect/°	(0–360°) Every 45° one class			

4.3.1. Influences of the Meteorological and Vegetation Factors on the FT Erosion Intensity

(1) Analysis of the FT erosion intensity at different annual temperature differences

Figure 9 shows the spatial distribution of the FT erosion area under different ATDs in the QTP. The results showed that FT erosion was mainly concentrated in regions with an ATD range of 19.2–29.2 °C, covering 86.11% of the total FT erosion area in the QTP. The moderate and strong FT erosion areas were mainly found in areas with an ATD range of 21.5–29.2 °C. Specifically, the strongest FT erosion intensities were observed in areas with an ATD range of 21.5–23.6 °C, and the moderate and strong FT erosion intensity areas covered 47.99% of the total FT erosion area in this ATD range (Figure 9). This ATD value range was observed in the mountain ranges, which were characterized by low AMPs and small ALT, as well as by steep slopes, high elevations, low NDVI, high soil–sand contents, and high MFDs, enhancing the FT erosion intensity.
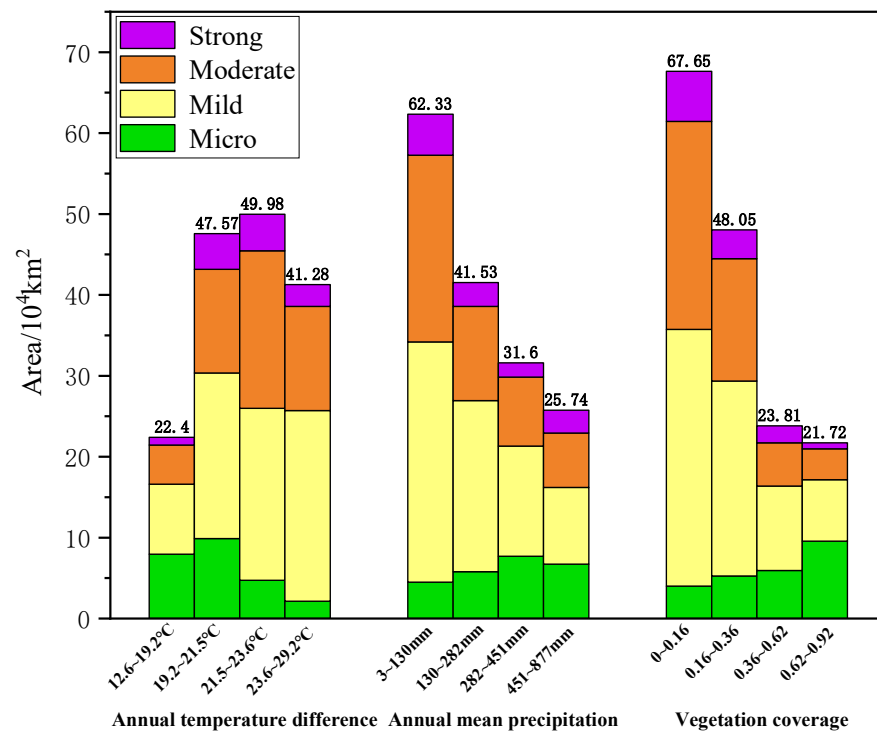
Figure 9. Effects of the meteorological and vegetation factors on the FT erosion intensity.

(2) Analysis of the FT erosion intensity at different annual mean precipitation amounts

Figure 9 shows the spatial distribution of the FT erosion area at different AMPs in the QTP. According to the obtained results, FT erosion in the QTP was mainly concentrated in areas with AMP ranging from 3 to 451 mm. In addition, 38.67% of the total FT erosion area in the QTP was observed in areas with an AMP range of 3–130 mm. The results highlighted an increase in the FT erosion intensity with increasing precipitation amount. According to Figure 9, it can be observed that the strong erosion is greatest at AMP of 451–877 mm, accounting for 10.91% of the total area of FT erosion in this precipitation zone. On the other hand, the moderate and strong FT erosion classes accounted for the highest proportion (45.15%) of the total FT erosion area with an AMP range of 3–130 mm. Areas with this precipitation amount range exhibited high FT erosion intensities, even though they were characterized by low AMPs and small active layer thicknesses. This finding might be attributed to the high ATDs, slopes, elevation, soil–sand contents, and MFDs, as well as to low NDVI values.

(3)   Analysis of the FT erosion intensity under different vegetation coverage

According to Figure 9, FT erosion in the QTP was mainly located in areas with NDVI values less than 0.36. The areas with NDVI values less than 0.16 accounted for 41.96% of the total FT erosion area in the QTP. Indeed, larger vegetation covers can provide an enhanced restriction of the FT erosion, thereby decreasing the FT erosion intensity. According to Figure 9, the proportions of the moderate and strong FT erosion areas showed decreasing trends with increasing NDVI value. The lowest FT erosion intensity was observed in areas with a NDVI value range of 0.62–0.92. Within this NDVI value range, the strong and moderate FT erosion class areas accounted for 3.45% and 17.6% of the total area of FT erosion in this NDVI zone, respectively.

4.3.2. Influences of the Topographical and Geomorphological Factors on the FT Erosion Intensity

(1)   Analysis of the FT erosion intensity at different slopes

The results indicated that FT erosion was mainly distributed in areas with slope degrees less than 13.58° (Figure 10), accounting for 95.26% of the total FT erosion area in the QTP. In addition, our results demonstrated an increasing trend of the FT erosion intensity with increasing slope degrees (Figure 10). Indeed, the highest FT erosion intensities were observed in areas with a slope range of 13.58–49.68°, while the strong and moderate FT erosion intensity classes accounted for 24.27% and 45.92% of the total FT erosion area within the 13.58–49.68° slope range, respectively.
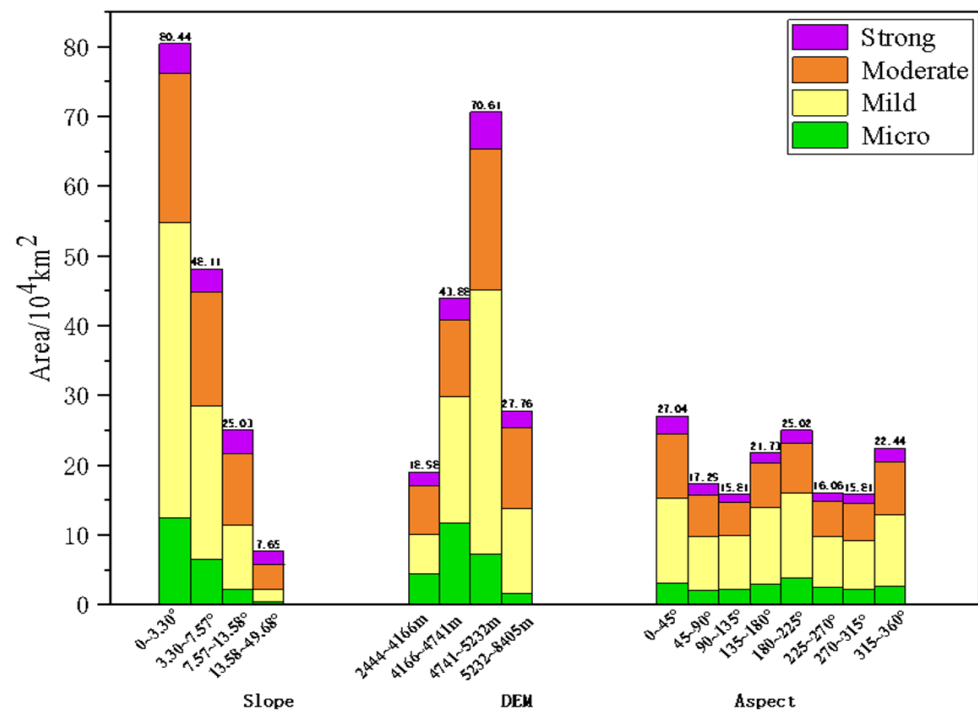
Figure 10. Influences of the topographical and geomorphological factors on the FT erosion intensity.

(2)   Analysis of the FT erosion intensity at different elevations

According to the obtained results, FT erosion was mainly distributed in areas with an elevation range of 4166–8405 m (Figure 10), covering 88.23% of the total FT erosion area in the QTP. The higher the elevation, the lower the temperature, and the higher the FT erosion intensity. The highest FT erosion intensities were observed in areas with an elevation range of 5232–8405 m (Figure 10). The moderate and strong FT erosion intensity classes covered 50.4% of the total FT erosion area within the 5232–8405 m elevation range.

(3)   Analysis of FT erosion intensity at different slope aspects

According to Figure 10, there were no substantial spatial differences in the FT erosion classes between the slope aspect classes in the QTP. In fact, different slope aspects can result in different solar radiation on soil surfaces, thereby influencing the FT erosion degree. However, the results revealed slight influences in the slope aspects on the FT erosion intensity in the study area. The FT erosion intensities at the different slope aspects belonged mainly to micro and mild erosion, accounting for about 60% of the total FT erosion areas within the different slope aspect ranges (Figure 10).

4.3.3. Influences of the Geological Factors on the FT Erosion Intensity

(1)   Analysis of the FT erosion intensity at different sand contents

According to the obtained results, the FT erosion intensities were mainly distributed in areas with soil–sand contents greater than 38% (Figure 11), covering 95.07% of the total FT erosion in the QTP. In general, the FT erosion intensity increased with increasing soil–sand contents. Indeed, the highest FT erosion intensities were observed in areas with a sand content range of 73–94%, while the strong and moderate FT erosion classes covered 11.68% and 43.5% of the total FT erosion within the 73–94% sand content range, respectively.
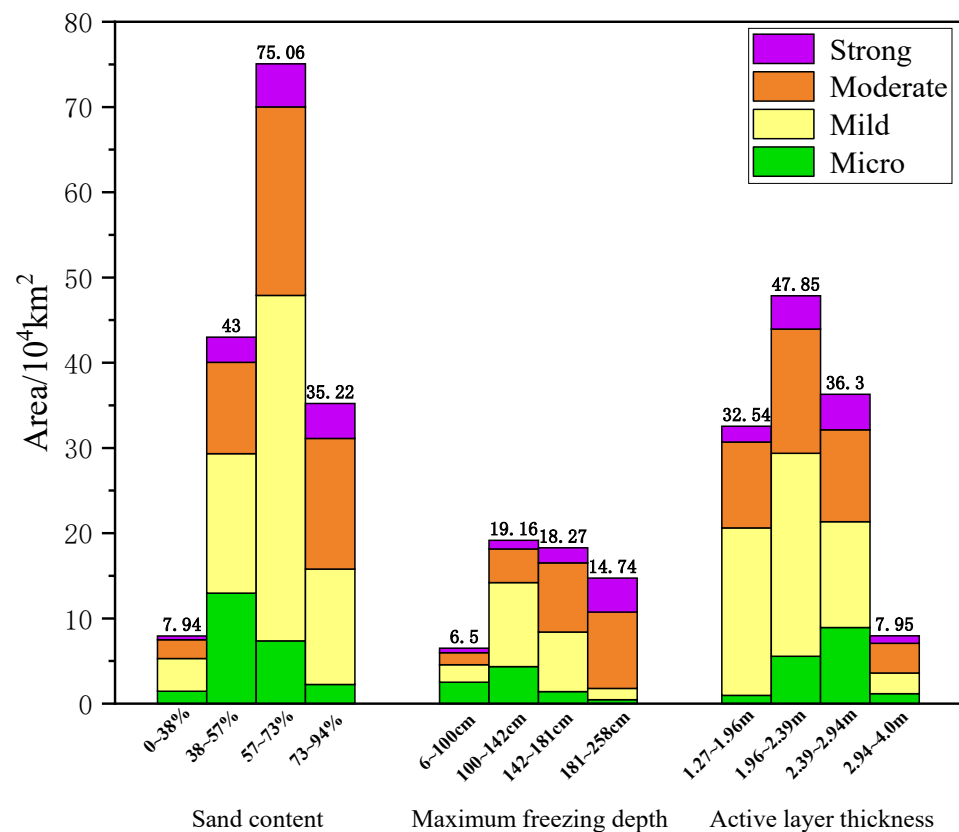
Figure 11. Influences of the geological factors on the freeze–thaw erosion intensity.

(2)   Analysis of the FT erosion intensity at different maximum freezing depths

The results revealed a widespread distribution of the FT erosion intensities areas with an MFD range of 100–258 cm (Figure 11), covering 88.93% of the total FT erosion areas in the QTP. Usually, high MFDs in seasonally permafrost areas can involve more soil masses in the FT erosion action, thereby increasing the occurrence likelihood of FT erosion events. According to Figure 11, the FT erosion intensity exhibited an increasing trend with increasing MFD. The 181–258 cm MFD range exhibited the highest FT erosion intensity, while the strong and moderate FT erosion areas covered 27.13% and 60.76% of the total FT

erosion area within the 181–258 cm MFD range, respectively. The moderate and strong FT erosion classes accounted for 33.83% of the total FT erosion area in the seasonally freezing zone. On the other hand, the micro and mild erosion classes covered 27.03 and 39.14% of the total FT erosion area, respectively.

(3)   Analysis of the FT erosion intensity at different active layer thicknesses

The FT erosion intensities were mainly observed in areas with an ALT range of 1.96–2.94 m (Figure 11), covering 67.52% of the total FT erosion area in the QTP. The obtained results in this study revealed a gradually increasing trend of the FT erosion intensity with increasing ALT (Figure 11). The highest FT erosion intensities were observed in areas with an ALT range of 2.94–4.0 m. In addition, the moderate and strong FT erosion classes accounted for 54.72% of the total FT erosion area within the 2.94–4.0 m ALT range. The moderate and strong FT erosion intensity classes covered 39.96% of the total FT erosion area in the multi-year FT erosion zone, whereas the micro and mild FT erosion intensity classes covered 12.47 and 47.57% of the total FT erosion area, respectively.

5. Discussion

The sources of FT erosion in the QTP are complex, as this type of erosion is influenced by a combination of meteorological, hydrological, topographical, pedological, and geological factors. Moreover, the QTP region is characterized by harsh climatic conditions, making it relatively difficult to conduct field studies. Indeed, the source and main mechanisms controlling the occurrence of FT erosion are still unclear. Moreover, besides the intensification of human activities, global warming and humidification have been intensified in recent years, resulting in glaciers and snow melting at high altitudes and, consequently, making FT erosion studies in the QTP region challenging. In addition, wang et al. [49] predicted widespread permafrost degradation as well as surface snow and ice melt on the QTP under future warming scenarios. In such an environment, the increase in FT hazards and the enhancement of FT erosion pose new problems for regional ecological restoration as well as engineering construction.

The QTP is the most widely distributed permafrost region in China. The permafrost is rich in underground ice and a large number of thermokarst phenomena, including thaw slumping and thermokarst lakes, which have occurred during the process of warming and humidification. According to Luo et al. [50] and Li et al. [51], a total of 2669 thaw-slumping sites and 120,374 thermokarst lakes have been observed in the QTP, of which FT erosion, induced by the direct exposure of subsurface ice due to thaw slumping, is the most abundant. Thermokarst lakes are dominated by the penetration of water bodies or the thawing and sinking of permafrost layers, resulting in obvious FT erosion edges. This thermokarst context can result in direct impacts on the environment and landscape. In addition, the occurrence of FT erosion events in the permafrost zone can promote carbon emissions, thereby enhancing climate warming [52]. Rocks and soils in the deep seasonally permafrost zone in the QTP can experience freezing and thawing cycles, leading to serious FT erosion, especially in some high and steep mountain areas. Therefore, the main factors induced in perennial and seasonally permafrost zones should be considered in future studies on FT erosion.

In this study, the FT erosion intensity in the QTP was semi-quantitatively analyzed using a comprehensive evaluation index. The obtained results of this study were assessed for accuracy by comparing them with those revealed in previous related studies. In general, the FT erosion intensity showed a decreasing trend with increasing NDVI. In contrast, increasing trends of the FT erosion intensity were observed with the increase in the remaining selected factors in this study. It should be noted that the highest FT erosion intensities were observed in areas with ATD and AMP values of the second and fourth levels, respectively. This finding further demonstrates the combined effect of multiple factors on FT erosion. For example, a small AMP range of 3–130 mm was mainly observed in the northwestern part of the QTP, where high ATDs, altitudes, soil–sand contents, and

slope degrees, as well as low NDVI values, were observed. Indeed, this part of the QTP exhibited the highest FT erosion intensities.

To accurately assess soil FT erosion, it is crucial to consider soil loss amounts per unit area per unit time in the FT erosion area [26]. However, there is still a few relevant data collected in China and other regions worldwide. The quantitative assessment of FT erosion on the QTP could be strengthened in subsequent studies. In addition, in this study, we classified the FT intensity and assessed their different influencing factors in the QTP without evaluating the evolution of FT erosion. But in the evaluation of FT erosion, factors such as MFD, ALT, thaw slumps, and rock glaciers were included, and the evaluation factors were comprehensive. This work can provide a reference for the prevention and control of soil FT erosion on the QTP, as well as for regional ecological environment protection and restoration. Future work can be related to the evolution of FT erosion in the QTP area, starting from long time-series high-resolution remote sensing data.

6. Conclusions

In this study, a total of 11 indicators, including ATD, AMP, slope, slope aspect, elevation, NDVI, sand content, MFD, ALT, thaw slump, and rock glacier, were selected and assigned AHP-based weights to assess the FT intensity in the QTP region using a comprehensive evaluation index method. The following conclusions were drawn:

(1) The total FT erosion area was 1.61×10^6 km^2, accounting for 61.33% of the total area of the QTP. The mild and moderate FT erosion intensity classes covered large areas of 7.33×10^5 and 4.94×10^5 km^2, accounting for 45.44% and 30.65% of the FT erosion total area in the QTP, respectively. On the other hand, the micro and strong FT erosion intensity classes were comparatively lower, covering 16.19% and 7.72% of the total FT erosion area in the QTP, respectively.

(2) The results revealed substantial variations in the spatial distribution of the FT erosion intensity in the QTP. The moderate and strong FT erosion intensity classes were observed mainly in the high mountain areas and the hilly part of the Hoh Xil frozen soil region. The southeastern, central, and western parts of the QTP were mainly characterized by the abundance of the micro and mild FT erosion intensity classes.

(3) The extent to which FT erosion intensity in the QTP was affected varies by the different evaluation indicators. The highest FT erosion intensities were observed in areas with an ATD range of 21.5–23.6 °C. In addition, the highest strong FT erosion proportions were found in areas with an AMP range of 451–877 mm, covering a total area of 10.91%. On the other hand, the slope aspect exhibited relatively small effects on the FT erosion intensity. The moderate and strong FT erosion area accounts for about 40% of each slope aspect zone in the QTP. In contrast, the highest FT erosion intensities were found in areas with an elevation range of 5232–5405 m. The results showed a decreasing trend of the FT erosion intensity proportion with increasing NDVI. However, increasing trends of the FT erosion intensity proportion were observed with increasing slope, sand content, MFD, and ALT.

Author Contributions: Conceptualization, Z.Y.; data curation, L.L. and S.R.; methodology, Z.Y. and F.N.; project administration, W.N. and F.N.; supervision, F.N. and W.N.; writing—original draft, Z.Y. and W.N.; writing—review and editing, Z.Y. and F.N. All authors have read and agreed to the published version of the manuscript.

Conflicts of Interest: The authors declare no conflicts of interest.

References

1. Zhang, J.; Liu, S.; Yang, S. Classification and assessment of freeze-thaw erosion in Tibet. *Acta Geogr. Sin.* **2006**, *61*, 911. [CrossRef]
2. Eigenbrod, K.D. Effects of cyclic freezing and thawing on volume changes and permeabilities of soft fine-gained soils. *Can. Geotech. J.* **1996**, *33*, 529–537. [CrossRef]
3. Zheng, M. Experimental Study on the Thawing and Sinking Characteristics of Seasonal Frozen Soil (Chalky Clay). Master's Thesis, Heilongjiang University, Harbin, China, 2012.
4. Wang, J.; Zhang, X.; Gulimire, F.; Wang, Z. Classification evaluation and spatial distribution characteristics of freeze-thaw erosion intensity in Heilongjiang Province of China. *Trans. Chin. Soc. Agric. Eng.* **2024**, *40*, 168–176.
5. Zhai, Y.; Fang, H. Spatiotemporal variations of freeze-thaw erosion risk during 1991–2020 in the black soil region, northeastern China. *Ecol. Indic.* **2023**, *148*, 110149. [CrossRef]
6. Chai, L.; Zhang, L.; Lv, X.; Hao, Z.; Liu, S. An investigation into the feasibility of using passive microwave remote sensing to monitor freeze/thaw erosion in China. *IEEE J. Sel. Top. Appl. Earth Obs. Remote Sens.* **2014**, *8*, 4460–4469. [CrossRef]
7. Sun, B.; Ren, F.; Ding, W.; Zhang, G.; Huang, J.; Li, J.; Zhang, L. Effects of freeze-thaw on soil properties and water erosion. *Soil Water Res.* **2021**, *16*, 205–216. [CrossRef]
8. Ferrick, M.G.; Gatto, L.W. Quantifying the effect of a freeze–thaw cycle on soil erosion: Laboratory experiments. *Earth Surf. Process. Landf. J. Br. Geomorphol. Res. Group* **2005**, *30*, 1305–1326. [CrossRef]
9. Williams, R.B.G.; Robinson, D.A. Experimental frost weathering of sandstone by various combinations of salts. *Earth Surf. Process. Landf. J. Br. Geomorphol. Res. Group* **2001**, *26*, 811–818. [CrossRef]
10. Wang, Q.; Qi, J.; Qiu, H.; Li, J.; Cole, J.; Waldhoff, S.; Zhang, X. Pronounced increases in future soil erosion and sediment deposition as influenced by Freeze–Thaw Cycles in the Upper Mississippi River Basin. *Environ. Sci. Technol.* **2021**, *55*, 9905–9915. [CrossRef] [PubMed]
11. Luo, J.; Niu, F.; Lin, Z.; Liu, M.; Yin, G. Recent acceleration of thaw slumping in permafrost terrain of Qinghai-Tibet Plateau: An example from the Beiluhe Region. *Geomorphology* **2019**, *341*, 79–85. [CrossRef]
12. Niu, F.; Luo, J.; Lin, Z.; Fang, J.; Liu, M. Thaw-induced slope failures and stability analyses in permafrost regions of the Qinghai-Tibet Plateau, China. *Landslides* **2016**, *13*, 55–65. [CrossRef]
13. Zhang, J.G.; Liu, S.Z. A new way for definiting the freezing-thaw erosion area in Tibet. *Geogr. Geo-Inf. Sci.* **2005**, *21*, 32–34.
14. Ouyang, Y.; Shen, W.S.; Yang, K.; Lin, N.F. The trend of freeze-thaw erosion in Yarlung Zangbo River Basin in nearly twenty years. *Mt. Res.* **2014**, *32*, 417–422.
15. Guo, B.; Zhou, Y.; Zhu, J.; Liu, W.; Wang, F.; Wang, L.; Jiang, L. An estimation method of soil freeze-thaw erosion in the Qinghai–Tibet Plateau. *Nat. Hazards* **2015**, *78*, 1843–1857. [CrossRef]
16. Lu, Y.; Liu, C.; Ge, Y.; Hu, Y.; Wen, Q.; Fu, Z.; Wang, S.; Liu, Y. Spatiotemporal characteristics of freeze-thawing erosion in the source regions of the Chin-Sha, Ya-Lung and Lantsang Rivers on the basis of GIS. *Remote Sens.* **2021**, *13*, 309. [CrossRef]
17. Zhang, J. Soil Erosion of the Buha River Basin Based on Remote Sensing and GIS. Master's Thesis, Qinghai Normal University, Xining, China, 2012.
18. Li, C.L.; Ma, J.H.; Tang, Z.G.; Zhou, W. GIS based evaluation on intensity of freeze-thaw erosion in head water region of the three river source area. *Soil Water Conserv. China* **2011**, *4*, 41–43.
19. Shi, Z.; Tao, H.; Liu, S.; Liu, B.; Guo, B. Research of freeze-thaw erosion in the Three-River-Source area based on GIS. *Trans. Chin. Soc. Agric. Eng.* **2012**, *28*, 214–221.
20. Wang, L.Y.; Xiao, Y.; Jiang, L.; Ouyang, Z.Y. Assessment and analysis of the freeze-thaw erosion sensitivity on the Tibetan Plateau. *J. Glaciol. Geocryol.* **2017**, *39*, 61–69.
21. Yu, W.; Zhao, L.; Li, Y.; Nan, Z.; Zhao, Y. Spatial-temporal variation of evapotranspiration based on the complementary relationship principle and its influencing factors on the Qinghai-Tibet Plateau. *Acta Ecol. Sin.* **2024**, *44*.
22. Huang, X. Spatio-Temporal Dynamic Evolution Analysis of Social-Ecological System Coupling and Ecological Risk Assessment—Take Tibetan Plateau as an Example. Master's Thesis, Chang'an University, Xi'an, China, 2023.
23. Fan, X.; Wang, Y.; Niu, F.; Li, W.; Wu, X.; Ding, Z.; Pang, W.; Lin, Z. Environmental Characteristics of High Ice-Content Permafrost on the Qinghai–Tibetan Plateau. *Remote Sens.* **2023**, *15*, 4496. [CrossRef]
24. Li, Z. Asphalt Mix Design and Performance Evaluation in Perennially Frozen Soil Area. Master's Thesis, Southeast University, Nanjing, China, 2005.
25. Zou, D.; Zhao, L.; Sheng, Y.; Chen, J.; Hu, G.; Wu, T.; Wu, J.; Xie, C.; Wu, X.; Pang, Q.; et al. A new map of permafrost distribution on the Tibetan Plateau. *Cryosphere* **2017**, *11*, 2527–2542. [CrossRef]
26. Zhang, J.G.; Liu, S.Z.; Fan, J.R. Identification and evaluation of freeze-thaw erosion in Sichuan province on the basis of GIS. *Mt. Res.* **2005**, *23*, 248–253.
27. Li, D. Distribution Laws of Erosion Intensity for the Three Soil Erosion Types in Gansu Province. Master's Thesis, Lanzhou University, Lanzhou, China, 2014.
28. Cui, J.; Xin, Z.; Huang, Y. The spatiotemporal variations in freeze-thaw erosion in 20032020 on the Qinghai-Tibet Plateau. *Acta Ecol. Sin.* **2023**, *43*, 4515–4526.

29. Guo, B.; Luo, W.; Wang, D.; Jiang, L. Spatial and temporal change patterns of freeze-thaw erosion in the three-river source region under the stress of climate warming. *J. Mt. Sci.* **2017**, *14*, 1086–1099. [CrossRef]
30. Fan, J.; Hu, T.; Yu, X.; Chen, J.; Han, L.; Zhou, Y. Evaluation of freeze–thaw erosion in Tibet based on the cloud model. *Front. Earth Sci.* **2021**, *15*, 495–506. [CrossRef]
31. Yao, T.D.; Qin, D.H.; Shen, Y.P.; Zhao, L.; Wang, N.L.; Lu, A.X. Cryospheric changes and their impacts on regional water cycle and ecological conditions in the Qinghai-Tibetan Plateau. *Chin. J. Nat.* **2013**, *35*, 179–186.
32. Lee, J.Y.; Lee, S. The frost penetration with the modified soil in the landfill bottom liner system. *Geosci. J.* **2002**, *6*, 7–12. [CrossRef]
33. Liu, X.; Cheng, Z.; Yan, L.; Yin, Z. Elevation dependency of recent and future minimum surface air temperature trends in the Tibetan Plateau and its surroundings. *Glob. Planet. Chang.* **2009**, *68*, 164–174. [CrossRef]
34. Zhou, Y.; Guo, D.; Qiu, G.; Cheng, G.; Li, S. *Permafrost in China*; Science Press: Beijing, China, 2000.
35. Okin, G.S.; Murray, B.; Schlesinger, W.H. Degradation of sandy arid shrubland environments: Observations, process modelling, and management implications. *J. Arid Environ.* **2001**, *47*, 123–144. [CrossRef]
36. Zhang, J.; Sha, Z.; Wang, J.; Qi, Y.; Chen, X.; Song, C. Freezing-thawing erosion in the Qinghai Lake basin based on remote sensing GIS. *J. Glaciol. Geocryol.* **2012**, *34*, 375–381.
37. Wang, S.L. Thaw slumping in Fenghuo Mountain area along Qinghai-Xizang highway. *J. Glaciol. Geocryol.* **1990**, *12*, 63–70.
38. Wang, Z.; Sha, Z.J.; Ma, Y.J.; Hu, J.F.; Zhai, Y.L.; Ma, H.Y. Intensity and spatial distribution characteristics of soil freeze-thaw erosion in alpine steppe region based on GIS. *J. Earth Environ.* **2017**, *8*, 55–64.
39. Yang, Z.; Ni, W.; Li, L.; Niu, F. Grading evaluation of muti factor soil freeze-thaw erosion intensity based on GIS—A case study of the upper reach of the Yangtze river. *J. Water Resour. Archit. Engnieering* **2022**, *20*, 89–95.
40. Meng, F.; Wang, Z.; Fu, Q.; Li, T.; Yang, X.; Zheng, E.; Zhang, G.; Zhuang, Q.; Fu, Q.; Zhang, Y. Study on the Change in Freezing Depth in Heilongjiang Province and Its Response to Winter Half-Year Temperature. *J. Appl. Meteorol. Climatol.* **2022**, *61*, 1003–1013. [CrossRef]
41. Wang, J.; Zhang, H.; Liu, Z.; Huang, B. Distribution of winter frozen soil depth in Qilian Mountain and its response to temperature change. In Proceedings of the 2009 IEEE International Geoscience and Remote Sensing Symposium, Cape Town, South Africa, 2–17 July 2009; Volume 2, pp. II–586–II–589.
42. Soons, J.M. Geocryology, a survey of periglacial processes and environments. *N. Z. Geogr.* **1979**, *37*, 43. [CrossRef]
43. Luo, J. *Distribution Data of Retrogressive Thaw Slump in Permafrost Zone of Qinghai-Tibet Plateau (2018–2020)*; National Tibetan Plateau/Third Pole Environment Data Center: Beijing, China, 2023.
44. Qiu, G.; Liu, J. *Dictionary of Permafrost (Chinese, English, Russian)*; Gansu Science and Technology Press: Gansu, China, 1994.
45. Wang, H.; Lin, Z.; Luo, J.; Li, N.; Li, P. *Rock Glacier Distribution at the Front of Glaciers in the Qinghai-Tibet Plateau, China (2022)*; National Tibetan Plateau/Third Pole Environment Data Center: Beijing, China, 2023.
46. Lu, Y.; Zhang, T.; Liu, Y.; You, Y.; Feng, C.; Kong, W. Evaluation and spatial distribution characteristics of freeze-thaw erosion intensity in the Yalu Tsangpo River basin on the basis of geographic information system. *Geomat. Nat. Hazards Risk* **2019**, *10*, 1047–1069. [CrossRef]
47. Jiao, C. Quantitative Assessment of Retrogressive Thaw Slump Induced Soil Erosion in Permafrost Regions on the Qinghai-Tibet Plateau. Ph.D. Thesis, South China University of Technology, Guangzhou, China, 2023.
48. Yin, G.; Luo, J.; Niu, F.; Lin, Z.; Liu, M. Machine learning-based thermokarst landslide susceptibility modeling across the permafrost region on the Qinghai-Tibet Plateau. *Landslides* **2021**, *18*, 2639–2649. [CrossRef]
49. Wang, T.; Yang, D.; Yang, Y.; Zheng, G.; Jin, H.; Li, X.; Yao, T.; Cheng, G. Pervasive permafrost thaw exacerbates future risk of water shortage across the Tibetan Plateau. *Earth's Future* **2023**, *11*, e2022EF003463. [CrossRef]
50. Luo, J.; Niu, F.; Lin, Z.; Liu, M.; Yin, G.; Gao, Z. Inventory and frequency of retrogressive thaw slumps in permafrost region of the Qinghai–Tibet Plateau. *Geophys. Res. Lett.* **2022**, *49*, e2022GL099829. [CrossRef]
51. Li, L. Study on the Evolution and Eco-Environmental Effects of Lakes in the Qinghai-Tibet Plateau. Ph.D. Thesis, Chang'an University, Xi'an, China, 2021.
52. Mu, C.C.; Abbott, B.W.; Norris, A.J.; Mu, M.; Fan, C.Y.; Chen, X.; Jia, L.; Yang, R.M.; Zhang, T.J.; Wang, K. The status and stability of permafrost carbon on the Tibetan Plateau. *Earth-Sci. Rev.* **2020**, *211*, 103433. [CrossRef]